Electrochemical Behavior of Monolayer and Bilayer Graphene

Anna. T. Valota,[†] Ian A. Kinloch,[‡] Kostya S. Novoselov,[§] Cinzia Casiraghi,[†] Axel Eckmann,[†] Ernie W. Hill,[⊥] and Robert A. W. Dryfe[†,*]

[†]School of Chemistry, [‡]School of Materials, [§]School of Physics & Astronomy, and [⊥]School of Computer Science, University of Manchester, Oxford Road, Manchester M13 9PL, United Kingdom

ABSTRACT Results of a study on the electrochemical properties of exfoliated single and multilayer graphene flakes are presented. Graphene flakes were deposited on silicon/silicon oxide wafers to enable fast and accurate characterization by optical microscopy and Raman spectroscopy. Conductive silver paint and silver wires were used to fabricate contacts; epoxy resin was employed as a masking coating in order to expose a stable, well-defined area of graphene. Both multilayer and monolayer graphene microelectrodes showed quasi-reversible behavior during voltammetric measurements in potassium ferricyanide. However, the standard heterogeneous charge transfer rate constant, k°, was estimated to be higher for monolayer graphene flakes.

KEYWORDS: graphene · electrochemistry · Raman spectroscopy · electron transfer

The unique charge transport properties of graphene have attracted enormous interest. Among the many conceived applications of graphene, there is also much interest in its use as an electrode material, with energy storage/conversion applications in mind. Examples include recent reports of graphene-based supercapacitors[1−3] and of the use of graphene as (almost) transparent electrodes in solar cells.[4−9] Optimization of such applications requires complete understanding of the electron transfer properties of graphene. However, despite a considerable amount of effort applied in this direction,[10−15] the understanding of the electrochemical activity of graphene remains controversial.[16] This work in fact feeds in to the considerable debate about the relative activity of the basal plane and edge planes of (bulk) graphitic samples.[17−21] Much of the lack of clarity about the electrochemical properties of graphene stems from the rather ill-defined sample preparation of almost all of the earlier reports on graphene electrochemistry: generally, graphene flakes (often a mixture of monolayer, bilayer and "other" samples) are simply dispersed on a conducting substrate, with no attempt made to isolate individual flakes, or to isolate the flake edges from the basal plane. Furthermore, the majority of studies to date have obtained graphene *via* chemical means, usually by reduction of graphene oxide, leaving doubts about the purity of the material.[22−24] There are a few notable exceptions to this general trend. Work on the capacitance of graphene has used a "top-gated" (effectively, electrochemical) configuration to bias the graphene/electrolyte interface.[25,26] More recently, work has appeared which describes the electrochemical properties of a single, masked flake in contact with an aqueous solution of a ferrocene derivative.[27] In the latter article, the authors noted an increase in electron transfer rate for the oxidation of the ferrocene derivative on the graphene sample, compared to values quoted on "bulk" graphite (highly oriented pyrolytic graphite, HOPG). The authors were unable to measure a rate constant for electron transfer on mechanically exfoliated graphene, the process was sufficiently fast that it was essentially reversible. A finite (slower) rate constant was determined on graphene prepared by chemical vapor deposition methods, this rate was still substantially higher than that measured on basal plane HOPG. The enhanced electron transfer kinetics seen on graphene were ascribed to the ripples present on its surface by the authors of this work. In this report, we have directly compared the voltammetric responses on a multilayer graphitic surface, with the response obtained for monolayer and bilayer graphene. Ferricyanide, which has been reported to show poor charge transfer kinetics on basal plane HOPG,[18,19] has been chosen as a model system to highlight differences in the behavior of the solids. Accordingly the first report of charge transfer kinetics on a monolayer graphene sample are presented, confirming that electron transfer kinetics are indeed improved on the graphene surface, relative to bulk graphitic materials.

* Address correspondence to robert.dryfe@manchester.ac.uk.

Received for review July 29, 2011 and accepted October 5, 2011.

Published online October 05, 2011
10.1021/nn202878f

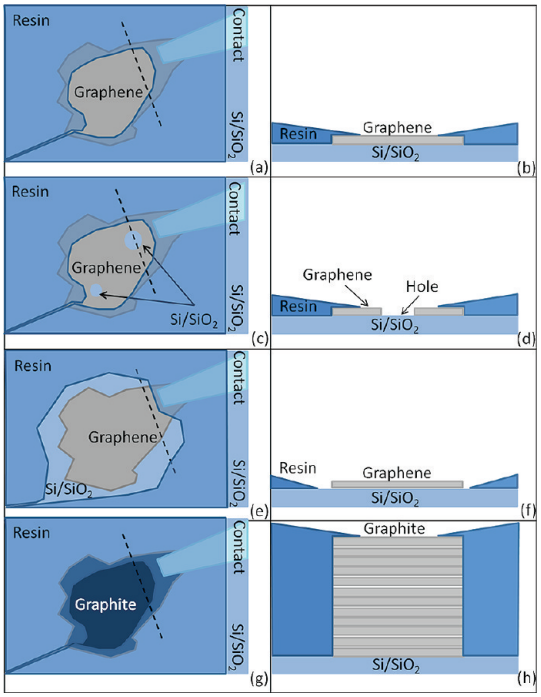

Figure 1. Schematic diagram of the samples employed in the present work. On the left, top view of the samples; on the right, cross section along the black dashed line. Samples are classified as defect-free monolayers, with all the edges covered by the masking resin (a, b); defective monolayers with evident holes (c, d); monolayers with exposed edges (e, f), and multilayers (g, h).

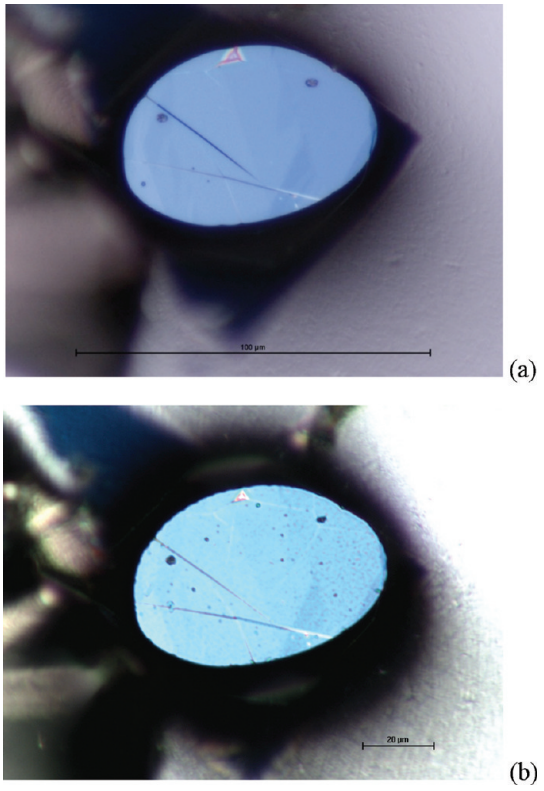

Figure 2. Optical micrographs of the multilayer sample before (a) and after (b) voltammetric experiments.

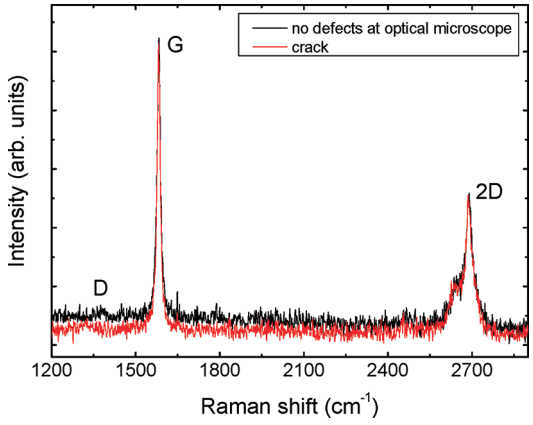

Figure 3. Raman spectra performed on two different spots on the multilayer graphene sample. Excitation wavelength, 633 nm; 50× objective; ~0.7 mW power (Renishaw spectrometer).

RESULTS

The reduction of aqueous phase ferricyanide was selected as our model redox process. A reduction process was chosen, to avoid the risk of oxidation of the graphene samples. Furthermore, a redox couple with a relatively low standard reduction potential was chosen to minimize any interference due to the reduction of the solvent background. The ferricyanide couple is interesting because it has been extensively investigated on carbon surfaces and is reported to have slow electron transfer kinetics on the basal plane of well-defined bulk graphitic phases (specifically, highly oriented pyrolytic graphite, HOPG).[19] A schematic diagram showing an overview of the analyzed samples is presented in Figure 1. Samples may be classified as defect-free monolayers, with all the edges covered by the masking resin (Figure 1a,b), defective monolayers with evident holes (Figure 1c,d), monolayers with exposed edges (Figure 1e,f) and multilayers, which for the purposes of this diagram means two or more layers (Figure 1g,h). Optical micrographs of a multilayer sample (>20 graphene sheets) are shown in Figure 2. Flakes of natural graphite were produced with a thickness varying from tens to hundreds of nanometers. AFM topography has previously revealed that steps and folds generated by cleavage of natural graphite are usually 10−20 nm high, with about one step edge every 800 nm.[28] Such defects are evident on the multilayer sample in Figure 2a, before exposure to the solution. Special attention was paid during masking of the samples in order to expose areas with the minimum number of defects; however, to date it has not been possible to achieve a perfect, edge-free region. However, Figure 2b indicates that no obvious change in the sample was observed following voltammetry. Raman spectra of the sample are presented in Figure 3. The voltammetric response observed on our multilayer sample is entirely consistent with previous literature reports for the ferri/ferrocyanide couple on

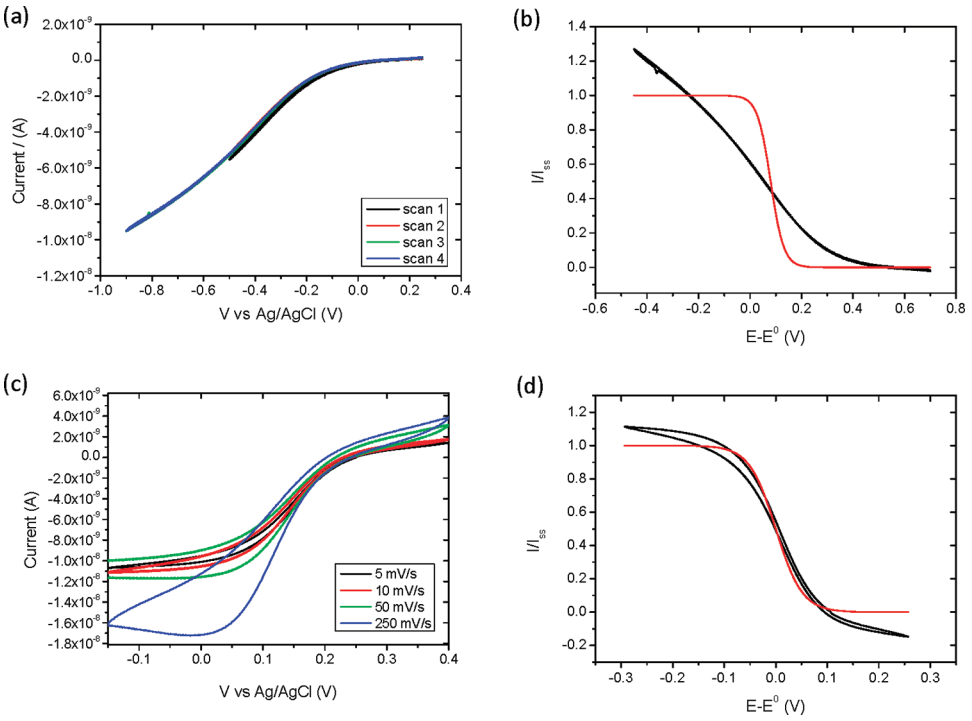

Figure 4. Voltammetric response of multilayer graphene at 5 mV/s (a) in 1 M KCl and 1 mM ferricyanide electrolyte; (b) the experimental data (black lines) is plotted along with the ideal response for reversible electron transfer (red lines). (c) The voltammetric data for various scan rates (see panel) is shown for the monolayer sample 1, the defect-free graphene; panel d applies the analysis performed for the multilayer sample in panel b to the 5 mV/s data from Sample 1. In both panels b and d, currents are normalized to the steady-state current.

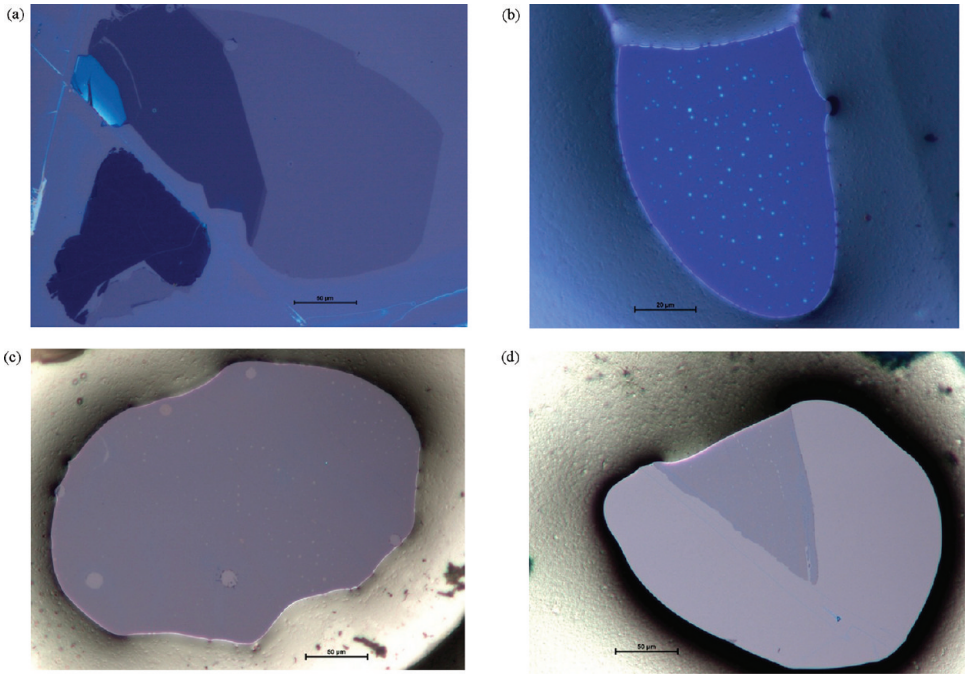

Figure 5. Optical micrographs of monolayer graphene samples. Sample 1 is shown before (a) and after (b) masking; in image b edges are completely masked. Sample 2 is shown to contain holes, in panel c; the exposed part of sample 3 is triangular, hence edges are exposed to solution (d).

(bulk) graphite and will be considered as our reference (see Figure 4a).[18,19] The limiting, background-subtracted current obtained at a scan rate of 5 mV s^{-1} was 7.5 nA. The predicted diffusion-limited current for an inlaid microdisc electrode varies between 6.2 and 9.5 nA, according to[29]

$$I_{lim} = 4nFDcr \quad (1)$$

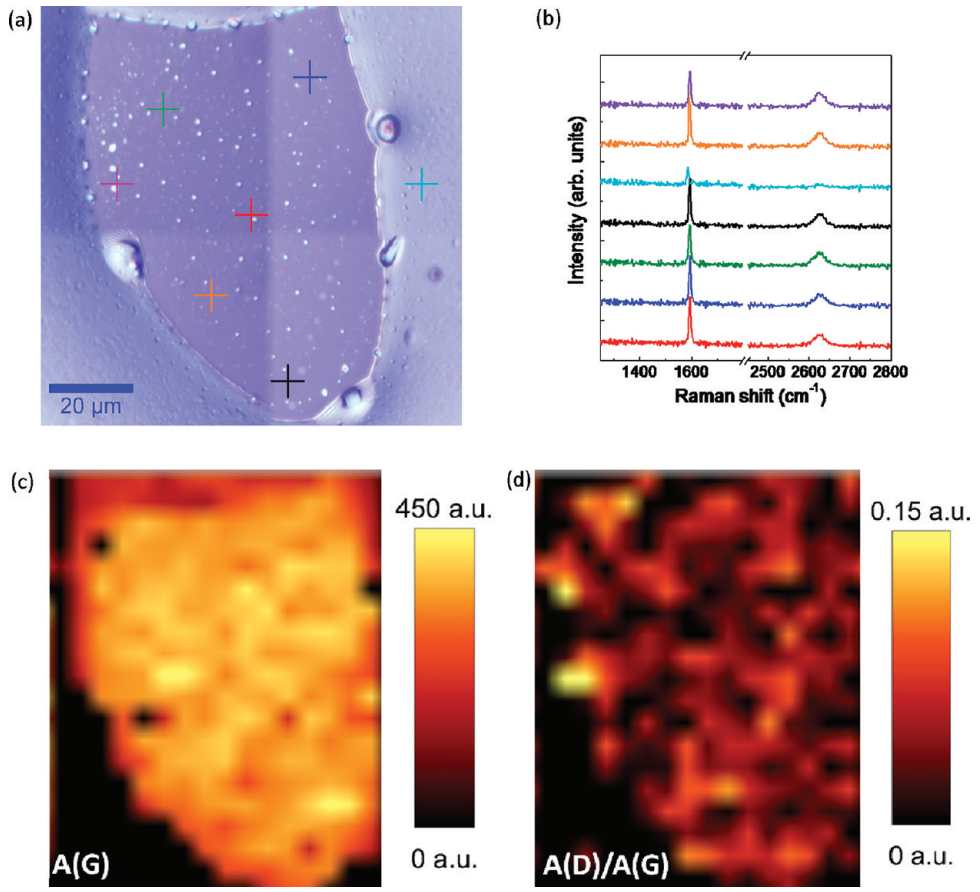

Figure 6. Optical image (a) and Raman spectra (b) performed on seven different spots on the defect-free monolayer graphene (Sample 1), after the first series of electrochemical measurements. Excitation wavelength, 633 nm; 100× objective; 0.7 mW laser power (Witec spectrometer). The crosses correspond to the locations where the mapping was performed; the colors of the crosses correspond to the colors of the Raman spectra. Map of the G peak integrated area (c) and of the ratio between the D peak and G peak integrated areas (d).

where n is the number of electrons exchanged in the redox reaction (1 in the present case), F is the Faraday constant, D is the diffusion coefficient of the electroactive species in solution (reported to vary between 5.37×10^{-6} cm^2 s^{-1} [30] and 8.20×10^{-6} cm^2 s^{-1} [31] for this solute), c is the bulk concentration of the ferricyanide, and r is the radius of the window to the solution. The standard electron transfer rate constant, k_0, for ferricyanide reduction on the multilayer graphite surface was calculated, from the procedure described by Mirkin and Bard,[32] to be 7×10^{-4} cm s^{-1}. Ferricyanide reduction on graphite has been widely studied in literature, most notably by McCreery and co-workers.[19,33] For HOPG with very low defect density, standard electron transfer rate constants lower than 10^{-6} cm s^{-1} were found. However, a 1% defect density is estimated to cause a 10^3 factor increase in k_0.[18]

The voltammetric responses of various monolayer graphene samples, which had different levels of defect visible, were investigated using the same redox couple (ferri/ferrocyanide, also shown in Figure 4). Micrographs of these samples are shown in Figure 5. Monolayer sample 1, shown in Figure 5a,b, contained no visible defects and its edges were completely masked, a conclusion supported by the fact that the ratio between the intensity of D and G peaks was lower than 0.1 in each point of the Raman map[34] (see Figure 6d). Before the masking process (Figure 5a), the surface of graphene Sample 1 appeared as homogeneous, with a characteristic color.[35] After masking was completed, the presence of bright dots was revealed by optical microscopy (Figure 5b). The nature of the observed dots, transparent to Raman spectroscopy (see Figure 6a,b) is unclear. However, the appearance of the dots just after the masking process indicates possible contamination of the graphene surface by epoxy particles.

Figure 7a shows the background voltammetric response of Sample 1 (masked, defect-free). Measurement of the non-Faradaic current density (at 0 V) as a function of sweep rate gives an estimate of the total interfacial capacitance per unit area, found to be 21.3 μF cm^{-2} (Figure 7b). In aqueous electrolytes, the total interfacial capacitance is composed of the quantum capacitance contribution from the graphene in series with the capacitance of the solution double layer, which can be resolved into a diffuse

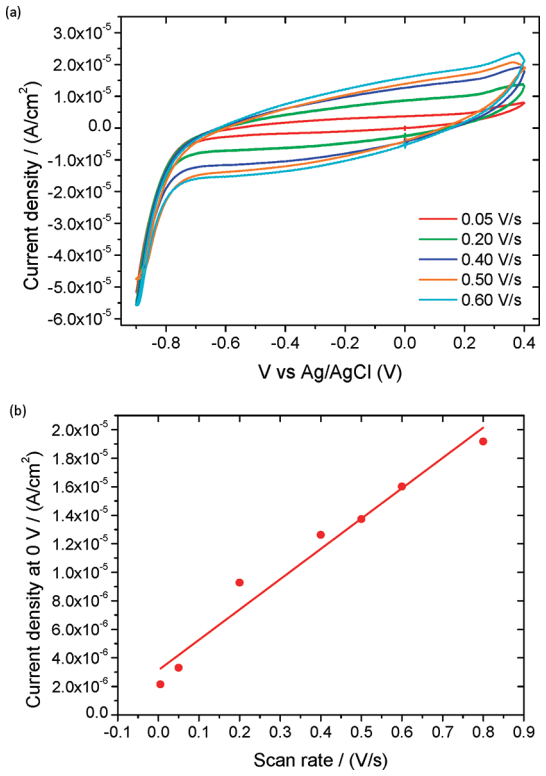

Figure 7. Current response of defect-free monolayer graphene (Sample 1) in background electrolyte (3 M aqueous solution of KCl) at various scan rates (a); plot of current density measured at 0 V *versus* scan rate (b). The gradient of the fitted line indicates a capacitance of 21.3 μF/cm^2.

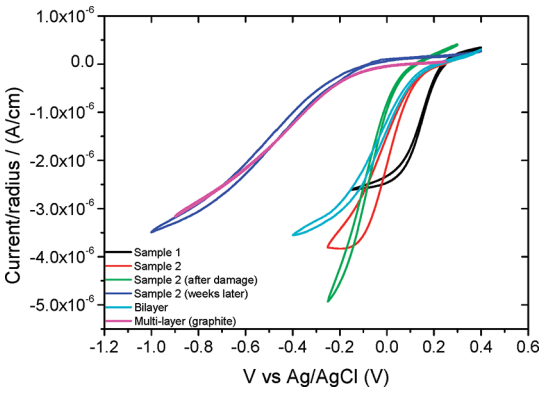

Figure 8. Current (normalized to electrode radius) *vs* potential response for the graphene monolayer samples (Samples 1 and 2), a bilayer sample and the multilayer.

and a compact component.[36] In the case of concentrated electrolytes such as the one used in the present work (3 M), the capacitance of the diffuse ionic layer is usually large (>100 μF cm^{-2}),[36] therefore its contribution to the total capacitance is negligible. The capacitance arising from the compact layer is known to have a value of about 10−20 μF cm^{-2},[36] suggesting that the value quoted above for the total interfacial capacitance is anomalously high. We note that capacitance of graphene has previously been quoted as between 8 and 10 μF cm^{-2} in 1 mM NaF aqueous solution, employing a.c. impedance spectroscopy, hence further investigation is required in order to clarify the aqueous phase capacitance behavior of monolayer graphene.[25]

Ferricyanide voltammetry at Sample 1 is shown in Figure 4c. As with the multilayer sample, the limiting current here (8.5×10^{-9} A), calculated *via* eq 1, is in reasonable agreement with the experimental value (9.6×10^{-9} A), assuming a ferricyanide diffusion coefficient of 5.4×10^{-6} cm^2 s^{-1}.[30] However, the current−potential response is more reversible than the multilayer graphite case, see Figure 4b,d, indicating that the graphene surface, despite its apparent lower level of defects, acts as an efficient catalyst for electron transfer from ferricyanide. A k_0 value of 1.2×10^{-3} cm s^{-1} was found for the monolayer sample (Sample 1), almost twice as high as the standard rate of electron transfer estimated with the (defect containing) multilayer.

As a matter of control we have also prepared samples with a number of defects. For instance, monolayer Sample 2 presented in Figure 5c contains several holes of *ca.* 10 μm diameter, hence some edge sites must be in contact with the electrolyte; the exposed part of monolayer Sample 3 is triangular (Figure 5d), hence edges are also exposed to solution in this case. Surprisingly, in view of received wisdom about the role of defects on electron transfer rates for bulk graphitic samples, the voltammetric responses of the defective monolayer samples (Samples 2 and 3) were not markedly different from that of the defect-free sample (Sample 1), at least for the case of ferricyanide reduction. Figure 8 presents the comparative current−potential response, where the current is normalized by sample radius to account for the different exposed windows of the monolayer samples (*c.f.*, eq 1). The current data obtained from a bilayer graphene sample is also presented, indicating that this material also presents electron transfer kinetics which are more similar to monolayer graphene than to the multilayer graphitic material.

It should be noted that the electron transfer kinetics obtained at the monolayer graphene samples degrade somewhat over a period of time. Figure 8 also shows the response from the monolayer Sample 2 (few holes, see Figure 5c) after a two week exposure to ambient conditions. The normalized current response is almost identical to that seen for the multilayer sample. A further feature we have observed is that defects on the graphene surface appear to act as nucleation sites for the fracture of samples under the influence of the applied potential. This phenomenon is obviously of interest and is the focus of ongoing work.

CONCLUSIONS

Monolayer and bilayer samples of graphene are electroactive and present improved electron transfer

kinetics, for the case of ferricyanide reduction, compared to the basal plane graphite substrates. Defects present on the monolayer make little difference to the voltammetric response of the samples.

EXPERIMENTAL METHODS

Fabrication of Electrodes. Samples of monolayer and bilayer graphene, and multilayer (>20 graphene sheets) graphite, were prepared by mechanical exfoliation of natural graphite supplied by NGS Naturgraphit GmbH. The samples were transferred to a silicon wafer, covered with a 90 nm thick thermal oxide layer. Conductive silver paint and silver wires were used to fabricate contacts. The samples were masked with an epoxy resin to leave a window of the order of 50 μm in diameter, deliberately exposing either the basal plane of each sample, or the basal plane and some of its edges. The precise dimensions of each exposed window were determined by optical microscopy. The samples were characterized by Raman spectroscopy, either using a Renishaw spectrometer (50× objective, ~0.7 mW power) or a Witec spectrometer (100× objective, ~0.6 mW power) at an excitation wavelength of 633 nm.

Chemicals and Electrochemical Apparatus. Voltammetric experiments were performed in aqueous solution using a three electrode configuration under potentiostatic control (Autolab PGSTAT30, Utrecht, The Netherlands). The masked graphene/graphite samples were used as the working electrode, an Ag/AgCl wire (prepared in-house) was used as the reference electrode, a Pt gauze was employed as the counter electrode. Water was obtained from an ELGA PureLab-Ultra purifier (minimum resistance 18.2 MΩ cm). For the electrolyte solutions, the redox active salt, $K_3Fe(CN)_6$, and the supporting electrolyte, KCl, were purchased from Sigma-Aldrich and Fisher-Scientific, respectively, and used as received. The pH of the freshly prepared ferricyanide electrolyte solution was 5.8 (Hanna Instruments pH meter).

Acknowledgment. We thank the U.K. EPSRC (Grants EP/I005145/1 and EP/G035954/1), the Royal Society, and the University of Manchester EPS strategic equipment fund for financial support. We thank J. Martin for assistance with preliminary experiments.

REFERENCES AND NOTES

1. Stoller, M. D.; Park, S.; Zhu, Y.; An, J.; Ruoff, R. S. Graphene-Based Ultracapacitors. *Nano Lett.* **2008**, *8*, 3498–3502.
2. Wang, Y.; Shi, Z.; Huang, Y.; Ma, Y.; Wang, C.; Chen, M.; Chen, Y. Supercapacitor Devices Based on Graphene Materials. *J. Phys. Chem. C* **2009**, *113*, 13103–13107.
3. Zhang, L. L.; Zhou, R.; Zhao, X. S. Graphene-Based Materials as Supercapacitor Electrodes. *J. Mater. Chem.* **2010**, *20*, 5983–5992.
4. Kumar, A.; Zhou, C. The Race to Replace Tin-Doped Indium Oxide: Which Material Will Win? *ACS Nano* **2010**, *4*, 11–14.
5. Choi, H.; Kim, H.; Hwang, S.; Han, Y.; Jeon, M. Graphene Counter Electrodes for Dye-Sensitized Solar Cells Prepared by Electrophoretic Deposition. *J. Mater. Chem.* **2011**, *21*, 7548–7551.
6. Wang, Y.; Chen, X.; Zhong, Y.; Zhu, F.; Loh, K. P. Large Area, Continuous, Few-Layered Graphene as Anodes in Organic Photovoltaic Devices. *Appl. Phys. Lett.* **2009**, *9*, 063302.
7. Wu, J.; Becerril, H. A.; Bao, Z.; Liu, Z.; Chen, Y.; Peumans, P. Organic Solar Cells with Solution-Processed Graphene Transparent Electrodes. *Appl. Phys. Lett.* **2008**, *92*, 263302.
8. Hecht, D. S.; Hu, L.; Irvin, G. Emerging Transparent Electrodes Based on Thin Films of Carbon Nanotubes, Graphene, and Metallic Nanostructures. *Adv. Mater.* **2011**, *23*, 1482–1513.
9. Hsieh, C. T.; Yang, B. H.; Lin, J. Y. One- and Two-Dimensional Carbon Nanomaterials as Counter Electrodes for Dye-Sensitized Solar Cells. *Carbon* **2011**, *49*, 3092–3097.
10. Chen, D.; Tang, L.; Li, J. Graphene-Based Materials in Electrochemistry. *Chem. Soc. Rev.* **2010**, *39*, 3157–3180.
11. Dan, Y.; Lu, Y.; Kybert, N. J.; Luo, Z.; Johnson, A. T. C. Intrinsic Response of Graphene Vapor Sensors. *Nano Lett.* **2009**, *9*, 1472–1475.
12. Robinson, J. T.; Perkins, F. K.; Snow, E. S.; Wei, Z.; Sheehan, P. E. Reduced Graphene Oxide Molecular Sensors. *Nano Lett.* **2008**, *8*, 3137–3140.
13. Alwarappan, S.; Erdem, A.; Liu, C.; Li, C. Z. Probing the Electrochemical Properties of Graphene Nanosheets for Biosensing Applications. *J. Phys. Chem. C* **2009**, *113*, 8853–8857.
14. Tang, L.; Wang, Y.; Li, Y.; Feng, H.; Lu, J.; Li, J. Preparation, Structure, and Electrochemical Properties of Reduced Graphene Sheet Films. *Adv. Funct. Mater.* **2009**, *19*, 2782–2789.
15. Zhou, M.; Zhai, Y.; Dong, S. Electrochemical Sensing and Biosensing Platform Based on Chemically Reduced Graphene Oxide. *Anal. Chem.* **2009**, *81*, 5603–5613.
16. Goh, M. S.; Pumera, M. The Electrochemical Response of Graphene Sheets Is Independent of the Number of Layers from a Single Graphene Sheet to Multilayer Stacked Graphene Platelets. *Chem. Asian J.* **2010**, *5*, 2355–2357.
17. Rice, R. J.; McCreery, R. L. Quantitative Relationship between Electron Transfer Rate and Surface Microstructure of Laser-Modified Graphite Electrodes. *Anal. Chem.* **1989**, *61*, 1637–1641.
18. Robinson, R. S.; Sternitzke, K.; McDermott, M. T.; McCreery, R. L. Morphology and Electrochemical Effects of Defects on Highly Oriented Pyrolytic Graphite. *J. Electrochem. Soc.* **1991**, *138*, 2412–2418.
19. Cline, K. K.; McDermott, M. T.; McCreery, R. L. Anomalously Slow Electron Transfer at Ordered Graphite Electrodes: Influence of Electronic Factors and Reactive Sites. *J. Phys. Chem.* **1994**, *98*, 5314–5319.
20. Banks, C. E.; Compton, R. G. Edge Plane Pyrolytic Graphite Electrodes in Electroanalysis: An Overview. *Anal. Sci.* **2005**, *21*, 1263–1268.
21. Edwards, M. A.; Bertoncello, P.; Unwin, P. R. Slow Diffusion Reveals the Intrinsic Electrochemical Activity of Basal Plane Highly Oriented Pyrolytic Graphite Electrodes. *J. Phys. Chem. C* **2009**, *113*, 9218–9223.
22. Shan, C.; Yang, H.; Song, J.; Han, D.; Ivaska, A.; Niu, L. Direct Electrochemistry of Glucose Oxidase and Biosensing for Glucose Based on Graphene. *Anal. Chem.* **2009**, *81*, 2378–2382.
23. Wang, J.; Yang, S.; Guo, D.; Yu, P.; Li, D.; Ye, J.; Mao, L. Comparative Studies on Electrochemical Activity of Graphene Nanosheets and Carbon Nanotubes. *Electrochem. Commun.* **2009**, *11*, 1892–1895.
24. Wu, J. F.; Xu, M. Q.; Zhao, G. C. Graphene-Based Modified Electrode for the Direct Electron Transfer of Cytochrome C and Biosensing. *Electrochem. Commun.* **2010**, *12*, 175–177.
25. Xia, J.; Chen, F.; Li, J.; Tao, N. Measurement of the Quantum Capacitance of Graphene. *Nat. Nanotechnol.* **2009**, *4*, 505–509.
26. Das, A.; Pisana, S.; Chakraborty, B.; Piscanec, S.; Saha, S. K.; Waghmare, U. V.; Novoselov, K. S.; Krishnamurthy, H. R.; Geim, A. K.; Ferrari, A. C. Monitoring Dopants by Raman Scattering in an Electrochemically Top-Gated Graphene Transistor. *Nat. Nanotechnol.* **2008**, *3*, 210–215.
27. Li, W.; Tan, C.; Lowe, M. A.; Abruña, H.; Ralph, D. C. Electrochemistry of Individual Monolayer Graphene Sheets. *ACS Nano* **2011**, *5*, 2264–2270.
28. Gu, J.; Leng, Y. Study of the Surface Topography of Graphite Materials Using Atomic Force Microscopy. *Carbon* **1999**, *37*, 991–994.

29. Bard, A. J.; Faulkner, L. R. *Electrochemical Methods: Fundamentals and Applications*; Wiley: New York, 1980.
30. Plana, D.; Jones, F. G. E.; Dryfe, R. A. W. The Voltammetric Response of Bipolar Cells: Reversible Electron Transfer. *J. Electroanal. Chem.* **2010**, *646*, 107–113.
31. Winkler, K. The Kinetics of Electron Transfer in Redox System on Platinum Standard-Size and Ultramicroelectrodes. *J. Electroanal. Chem.* **1995**, *388*, 151–159.
32. Mirkin, M. V.; Bard, A. J. Simple Analysis of Quasi-Reversible Steady-State Voltammograms. *Anal. Chem.* **1992**, *64*, 2293–2302.
33. Kneten, K. R.; McCreery, R. L. Effects of Redox System Structure on Electron-Transfer Kinetics at Ordered Graphite and Glassy Carbon Electrodes. *Anal. Chem.* **1992**, *64*, 2518–2524.
34. Casiraghi, C.; Hartschuh, A.; Qian, H.; Pliscanec, S.; Georgia, C.; Fasoli, A.; Novoselov, K. S.; Basko, D. M.; Ferrari, A. C. Raman Spectroscopy of Graphene Edges. *Nano Lett.* **2009**, *9*, 1433–1441.
35. Blake, P.; Hill, E. W.; Castro Neto, A. H.; Novoselov, K. S.; Jiang, D.; Yang, R.; Booth, T. J.; Geim, A. K. Making Graphene Visible. *Appl. Phys. Lett.* **2007**, *91*, 063124.
36. Randin, J.-P.; Yeager, E. Differential Capacitance Study of Stress-Annealed Pyrolytic Graphite Electrodes. *J. Electrochem. Soc.* **1971**, *118*, 711–714.